



HAL
open science

Interpolations of Geo Spatial Variables using Mathematical Morphology

Aditya Challa, Sravan Danda, B S Daya Sagar, Laurent Najman

► **To cite this version:**

Aditya Challa, Sravan Danda, B S Daya Sagar, Laurent Najman. Interpolations of Geo Spatial Variables using Mathematical Morphology. 2017. hal-01484894v1

HAL Id: hal-01484894

<https://hal.science/hal-01484894v1>

Preprint submitted on 8 Mar 2017 (v1), last revised 9 Jan 2018 (v3)

HAL is a multi-disciplinary open access archive for the deposit and dissemination of scientific research documents, whether they are published or not. The documents may come from teaching and research institutions in France or abroad, or from public or private research centers.

L'archive ouverte pluridisciplinaire **HAL**, est destinée au dépôt et à la diffusion de documents scientifiques de niveau recherche, publiés ou non, émanant des établissements d'enseignement et de recherche français ou étrangers, des laboratoires publics ou privés.

Interpolations of Geo Spatial Variables using Mathematical Morphology

Aditya Challa, *Member, IEEE*, Sravan Danda, *Member, IEEE* B. S. Daya Sagar, *Senior Member, IEEE* and Laurent Najman

Abstract—The problem of interpolation of images is defined as - given two images at time $t = 0$ and $t = T$, one must find the series of images for the intermediate time. This problem is not well posed, in the sense that without further constraints, there might be many solutions possible. However, restricting the domain of application allows us to choose the “right” solution. We thus focus on the interpolation problem from the perspective of geoscience and remote sensing. One approach to obtain a solution to image interpolation problem is with the use of operators from Mathematical Morphology (MM). These operators have an advantage of preserving the structure since the operators are defined on sets. In this work we review and consolidate existing solutions to the image interpolation problem from the perspective of geoscience and remote sensing. We also summarize several possible extensions and prospective problems of current interest.

Index Terms—Image Interpolation, Mathematical Morphology, Morphological Interpolation.

I. INTRODUCTION

THE problem of image interpolation can be stated as - given two Images I_0 and I_1 , find the series of Images $\{Z_\alpha, \alpha \in [0, 1]\}$ such that $Z_0 = I_0$ and $Z_1 = I_1$. Note that this problem differs from the usual interpolation problem - given a function values at few points, find the value of the function at the intermediate points. Image interpolation problem requires the answers to be “visually appealing” which is very hard to characterize rigorously. For instance in figure 1, let the source image be as in (a) and target image be as in (b). A simple linear interpolation $(0.5 * I_0 + 0.5 * I_1)$ would result in the one as obtained in (c). However, we expect that the “structure” to change from the circle to square.

Image interpolation problem is also sometimes referred to as *Image morphing* which is widely used for special effects and animation. In this work, our aim is to analyze the problem from the perspective of remote sensing and geoscience and, as we shall soon see, the nature of the solutions are very different from that of Image morphing. Several possible applications exist for such a solution. For example, a satellite maps the surface at regular intervals and one might be interested in visualizing the intermediate states. Apart from this the problem of image interpolation is of interest to the Geographic Information Systems (GIS) community [1].

The solution to the image interpolation problem can be approached from various starting points. In this work, we

Aditya Challa, Sravan Danda and B.S.Daya Sagar are with the Systems Science and Informatics Unit, Indian Statistical Institute, Bangalore.

Laurent Najman is with Université Paris-Est, LIGM, Equipe A3SI, ESIEE, France.

are interested in analyzing the solution obtained via the use of operators from *Mathematical Morphology* (MM). MM is a theory of non-linear operators on images introduced by Georges Matheron and Jean Serra in the late seventies [2]. These operators are famous for preserving the “structure” as the operators are defined on sets instead of pixels. This makes the subject of morphological operators ideal to deal with the problem of image interpolation. The question of why MM operators are ideal for interpolation of geo-spatial variables will be discussed further in section II-E.

Different solutions to the problem of image interpolation via MM operators are proposed in several works [3], [4]. One of the aims of this article is to provide a consolidated theoretical review of the earlier methods from the geoscience and remote sensing perspective. We also discuss several extensions and prospective problems for future work.

The main contributions of this article are -

- Theoretical consolidation of the existing methods
- Analysis of existing methods through simple, simulated examples.
- Provide a platform for various extensions and future work.

The methods described in this article are not the only possible solutions to the interpolation problem [5], [6], [3].

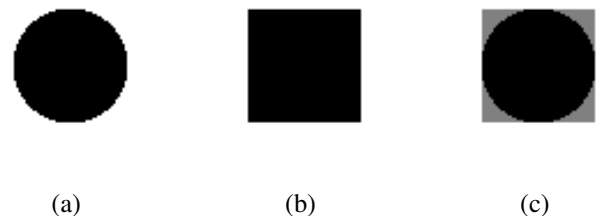


Fig. 1. (a) Source Image. (b) Target Image. (c) Linear interpolation between (a) and (b).

II. REVIEW OF MORPHOLOGICAL OPERATORS

In this section we introduce the basic operators of Mathematical Morphology (MM), recall the definitions and setup the notation as required by the rest of the article [7], [8], [9].

Loosely speaking, the basic MM operators - *dilation*, *erosion*, *opening* and *closing*, are defined on binary images and can be extended to greyscale images. This is achieved on the abstract level by defining the operators on abstract structures

called *Complete Lattices*. However, for the purposes of this article, we only review the basic operators on binary and greyscale images. Interested readers can refer to [7], [8] for theoretical details on MM operators and [10], [11] for details about lattices.

A. Binary Images

A binary image is a map, $I : E \rightarrow \{0, 1\}$. E is called the *domain of definition* and is usually taken as \mathbb{R}^2 or \mathbb{Z}^2 . Here \mathbb{R} refers to the real line and \mathbb{Z} denotes the set of integers. For most of theoretical aspects in this article, we consider $E = \mathbb{R}^2$. Note that, practically, images are restricted to a finite domain. However results, henceforth, are stated on infinite domain and hold true for finite domains as well. This distinction is blurred for the rest of the article for pedagogical reasons.

An equivalent way of characterizing the binary image is to look at sets $\{x \in E \mid I(x) = 1\}$. Such sets belong to the space of $\mathbb{P}(E)$, where $\mathbb{P}(E)$ is the power set - set of all possible subsets of E . Basic MM operators on binary are maps from $\mathbb{P}(E) \rightarrow \mathbb{P}(E)$. To define these operators one needs another set, called *structuring element*, with a defined origin.

There are several ways to look at the structuring element. Theoretically, a structuring element is the set to which the set $\{0\}$ maps to. Then using the assumption - *Invariance to translation*, we can extend the mapping to all unit sets $\{x\}$. Then using the assumption - *Invariance to supremum* gives us the dilation and using the assumption - *invariance to infimum* gives us erosion. For the remaining part of the paper it is assumed that B denotes a unit disk with origin at the center.

1) *Dilation*: The first MM operator we discuss is that of *Morphological Dilation*, or simply *Dilation*, $\delta_B(\cdot)$. Recall that it is a map from $\mathbb{P}(E)$ to itself. Thus we have

$$\delta_B(X) = X \oplus B = \bigcup_{b \in B} X_b = \{x \in E \mid B_x \cap X \neq \emptyset\}, \quad (1)$$

where $X \oplus B$ is usual Minkowski addition and X_b is the set X translated by b .

2) *Erosion*: *Morphological Erosion*, or simply *Erosion*, $\epsilon_B(\cdot)$ with respect to the structuring element B is defined as

$$\epsilon_B(X) = X \ominus \hat{B} = \bigcap_{b \in B} X_{-b} = \{x \in E \mid B_x \subseteq X\}, \quad (2)$$

where $X \ominus B$ is usual Minkowski subtraction. When the dilations and erosions are restricted to a domain, they are called *Geodesic Dilations* and *Geodesic Erosions* respectively. Assume that we have two sets $X \subset Y$. The geodesic dilation and geodesic erosion are respectively defined by

$$\Delta_{Y,B}(X) = \delta_B(X) \cap Y \quad (3)$$

$$\mathcal{E}_{X,B}(Y) = \epsilon_B(Y) \cup X \quad (4)$$

B. Greyscale Images

A greyscale image is defined as a function $I : \mathbb{R}^2 \rightarrow \overline{\mathbb{R}}$, where $\overline{\mathbb{R}} = \mathbb{R} \cup \{-\infty, \infty\}$. An equivalent way of looking at the greyscale image is using the *umbra* [8] defined as

$$U(I) = \{(x, t) \mid I(x) \leq t\} \quad (5)$$

Note that $U(I) \subset \mathbb{R}^3$. Using these sets, the definitions of dilation and erosion for binary images can be extended to greyscale images as well. The main distinction being how the structuring element is extended from \mathbb{R}^2 to \mathbb{R}^3 .

The most important point to note is that - all dimensions are not created equal. Observe that two dimensions correspond to the spatial co-ordinates while the third corresponds to the greyscale value. The spatial co-ordinates can be handled the same way as before. The greyscale value on the other hand, can be handled in two ways - with/without changing the maximum greyscale value in the image. This results in *non-flat* and *flat* structuring elements respectively.

1) *Flat Structuring Elements*: Given a set $B \subset \mathbb{R}^2$, a flat structuring element is defined as

$$g(x) = \begin{cases} 0 & x \in B \\ -\infty & x \notin B \end{cases} \quad (6)$$

2) *Non-Flat Structuring Elements*: Given a set $B \subset \mathbb{R}^2$, a non-flat structuring element is defined as

$$g(x) = \begin{cases} i_x & x \in B \\ -\infty & x \notin B \end{cases} \quad (7)$$

where i_x can take any value in \mathbb{R} .

3) *Greyscale Operators*: *Greyscale Morphological Dilation* with respect to the structuring element $g(x)$, $\delta_g(\cdot)$ is defined as

$$\delta_g(f)(x) = \sup\{f(h) + g(x - h) \mid h \in E\} \quad (8)$$

Greyscale Morphological Erosion with respect to the structuring element g , $\epsilon_g(\cdot)$ is defined as

$$\epsilon_g(f)(x) = \inf\{f(h) - g(x - h) \mid h \in E\} \quad (9)$$

The importance of the distinction between flat and non-flat structuring elements and greyscale operators are further discussed in section (refer). Unless otherwise mentioned, in what follows the dilation and erosion operators refer to operators on binary images.

C. Hausdorff Distances

Another concept used in the remaining portion of the article is that of distance between sets. There are various distances which can be defined on two sets. *Dilation distance*, $\bar{d}(X, Y)$ is defined as $\inf\{\lambda \mid \delta_{\lambda B}(X) \supseteq Y\}$. *Hausdorff Dilation distance* is defined as $d(X, Y) = \sup\{\bar{d}(X, Y), \bar{d}(Y, X)\}$. The following are the list of properties which follow from the definition -

- 1) $d(X, Y) = d(Y, X)$
- 2) $d(X, Y) = 0$ if and only if $X = Y$.
- 3) $d(X, Y) \leq d(X, Z) + d(Y, Z)$.
- 4) If we have that $X \subseteq Y$, then $d(X, Y) = \bar{d}(X, Y)$

We can also define the “dual” distance operator, *Erosion distance* as $\bar{e}(X, Y)$ is defined as $\inf\{\lambda \mid \epsilon_{\lambda B}(X) \subseteq Y\}$. And the *Hausdorff Erosion distance* is defined as $e(X, Y) = \sup\{\bar{e}(X, Y), \bar{e}(Y, X)\}$.

D. Influence Zones

If Z_1 and Z_2 are two sets in \mathbb{R}^2 , then the influence zone of Z_1 with respect to Z_2 is defined as

$$IZ(Z_1 | Z_2) = \{x : \bar{d}(Z_1, x) < \bar{d}(Z_2, x)\} \quad (10)$$

Similarly, influence zone of Z_2 with respect to Z_1 is defined as

$$IZ(Z_2 | Z_1) = \{x : \bar{d}(Z_2, x) < \bar{d}(Z_1, x)\} \quad (11)$$

One can give a simpler characterization for the influence zone. Fix a point x . Now $x \in IZ(Z_1 | Z_2)$ if and only if we have that $x \in Z_1 \oplus \lambda B$ and $x \notin Z_2 \oplus \lambda B$. That is $x \in (Z_2 \oplus \lambda B)^c$. Thus we have

$$IZ(Z_1 | Z_2) = \bigcup_{\lambda \geq 0} (Z_1 \oplus \lambda B) \cap (Z_2 \oplus \lambda B)^c \quad (12)$$

We can also define the *Skeleton by Influence Zone (SKIZ)* as

$$SKIZ(Z_1, Z_2) = \{x : d(Z_2, x) = d(Z_1, x)\} \quad (13)$$

E. Interpolation of Geo-Spatial Variables

1) *Why Geo-Spatial variables?:* Considering images as points in \mathbb{R}^{n^2} , where n^2 is the number of pixels in the image, the problem of image interpolation can be restated as - Find a path in \mathbb{R}^{n^2} between two points. This problem, of course, has infinitely many solutions. To get a unique solution, one needs to place some constraints on the paths. Usual constraints are 1) the path should be smooth and 2) the interpolates visually appealing. However, “visually appealing” is very hard to characterize. Instead constraining the data domain can allow to pick a unique path. Thus, in this article we focus on geo-spatial variables.

2) *Advantage of MM operators:* Recall that MM operators (Binary) act by increasing/decreasing the set of pixels. This means that they act by changing the structure of the set, and hence one has a control over the structure. As noted in section I, we expect the solution to the interpolation problem to act on the structure of the set. The images in figure 2 are generated using geodesic dilation. Contrasting them with that of figure 1 we find that interpolates in figure 2 are “smoother”.

3) *Why MM operators on Geo-Spatial variables?:* Apart from the fact that MM operators operate on the structure of the sets, they also simulate many geophysical processes. This is another reason why MM operators are ideal for interpolating Geo-spatial variables. For instance constrained water flow can be simulated by geodesic dilation.

III. FIRST ATTEMPTS

In this section we review the two methods as described in [4]. Recall that we are interested in constraints so that we can pick uniquely the path between the two images. One such constraint is given by Hausdorff distances.

Rigorously speaking, consider the space \mathcal{K} of all non empty compact sets, with the metric given by Hausdorff distance. If

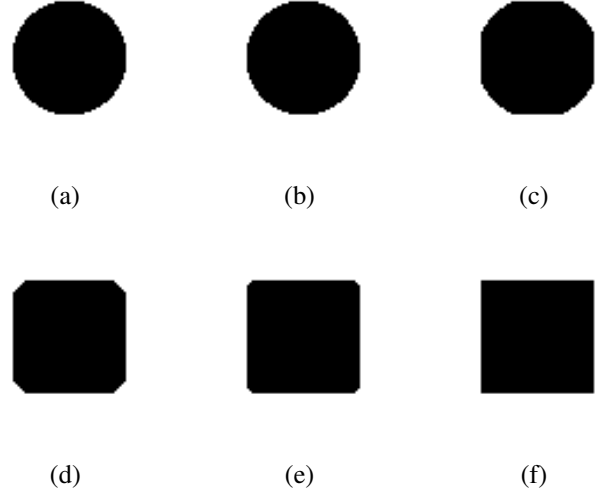


Fig. 2. (a) Source Image. (b) - (e) Geodesic Dilation. (f) Target Image.

X and Y are two sets, then we shall be interested in shortest path between X and Y in this space. One of the shortest paths is given by the *First Hausdorff Interpolates* defined below.

Definition 1 (First Hausdorff Interpolates). *Let X and Y be two sets. Let $\rho = d(X, Y)$ (Hausdorff distance). Let B denote the disk structuring element with radius 1. Then the first Hausdorff interpolates, $\{Z_\alpha : \alpha \in [0, 1]\}$ is defined as*

$$Z_\alpha = \delta_{\alpha\rho B}(X) \cap \delta_{(1-\alpha)\rho B}(Y) \quad (14)$$

The interpolates defined in definition 1 satisfy

$$d(Z_\alpha, X) = (\alpha)\rho \quad d(Z_\alpha, Y) = (1 - \alpha)\rho \quad (15)$$

The proof of this can be found in [4]. The above relation implies that the first Hausdorff interpolates falls on the shortest path between the sets X and Y .

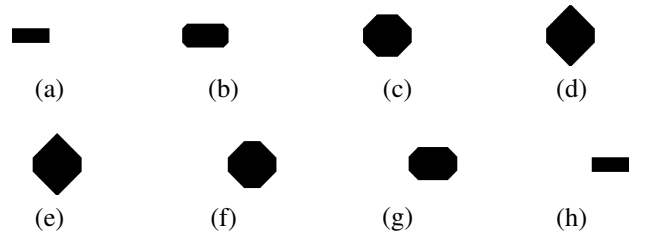


Fig. 3. First Hausdorff Interpolates. (a) Source Image. (b) - (g) First Hausdorff Interpolate. (h) Target Image.

An example of the first Hausdorff interpolate is given in figure 3. It is observed that these interpolates even though theoretically sound, suffer from the problem of “thick” interpolates as illustrated in figure 3. There are two ways around this problem - 1) Observe that the sets X and Y are simple translations of each other. Thus negating the affine transformations might reduce this effect. 2) Or more simply, we can restrict the interpolates to the convex hull of sets X and Y . This also reduces the problem of “thick” interpolates.

Definition 2 (Second Hausdorff Interpolates). *Let X and Y be two sets. Let $\rho = d(X, Y)$ (Hausdorff distance). Let B denote the disk structuring element with radius 1. Then the first hausdorff interpolates, $\{Z_\alpha : \alpha \in [0, 1]\}$ is defined as*

$$Z_\alpha = \delta_{\alpha\rho B}(X) \cap \delta_{(1-\alpha)\rho B}(Y) \cap ((1-\alpha)X \oplus (\alpha)Y) \quad (16)$$

The second method above makes up the *Second Hausdorff Interpolates* as defined in definition 2. The corresponding second Hausdorff interpolates for figure 3 are shown in figure 4.

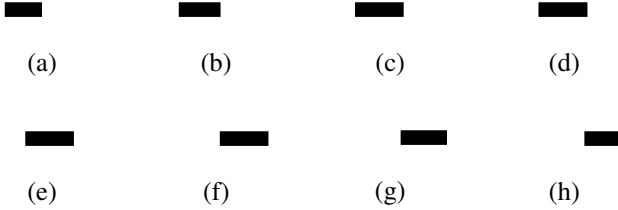


Fig. 4. Second Hausdorff Interpolates. (a) Source Image. (b) - (g) Second Hausdorff Interpolate. (h) Target Image.

IV. INTERPOLATIONS THROUGH MEDIAN

In this section we look at yet another method to calculate the interpolates. To start with we propose a series of simplifications which reduces and simplifies the problem of finding image interpolates, and then propose a solution which does so. We also analyze various properties and explain their significance. This section is a consolidation of ideas from [3], [4], [12], [13].

A. Series Of Simplifications

Here, we reduce to the problem of finding image interpolates to a simpler problem, which would be easier to solve. We assume binary images, which are equivalent to sets in $\mathbb{P}(E)$. We assume in this section that the problem is to find the interpolates between sets X and Y .

1) $X \cap Y \neq \emptyset$: Consider the case when a set X is deformed by a translation in space to $X_h = X + \{h\}$. The ideal interpolates must be of that of a translation, i.e $Z_\alpha = X + \{\alpha h\}$. Morphological operators are not equipped to handle such transformations. Indeed, the dilation and erosion operators are extended assuming translation to invariance. Hence, if the operators assume translation invariance, they cannot simulate translation. Hence it makes sense to “negate” the translation before calculating the interpolates and then adjust the solution accordingly. Infact we “negate” all affine transformations.

Proposition 1. *Let \mathcal{T} denote an affine transformation. Let X and Y be two sets. If $\mathcal{T}(X) \cap Y = \emptyset$ for all \mathcal{T} then either X is empty or Y is empty.*

The above proposition is easy to see. Proposition 1 and negating the affine transformations allows the assumption

$$X \cap Y \neq \emptyset \quad (17)$$

to hold true. The “ideal” affine transformation is obtained by

$$\mathcal{T}^* = \arg \max Area(\mathcal{T}(X) \cap Y) \quad (18)$$

the affine transformation which maximizes the area of intersection between X and Y . To solve this is hard, but there exists several approximations [12]. We assume that any affine transformation has 3 parts - translation, rotation and scaling, that is

$$\mathcal{T} = T_h R_\theta S_\lambda \quad (19)$$

We can accordingly define,

$$\mathcal{T}^{-(1-\alpha)} = T_{-(1-\alpha)h} R_{-(1-\alpha)\theta} S_{-(1-\alpha)\lambda} \quad (20)$$

How to reconstruct the Interpolates? Let interpolates between $\mathcal{T}(X)$ and (Y) be $\{Z'_\alpha\}$. Then the interpolates between X and Y is obtained by

$$Z_\alpha = \mathcal{T}^{-(1-\alpha)}(Z'_\alpha) \quad (21)$$

To check this, observe that $Z_0 = \mathcal{T}^{-(1)}(Z'_0) = \mathcal{T}^{-(1)}\mathcal{T}(X) = X$. And similarly we have $Z_1 = Y$.

2) $X \subseteq Y$: Intuitively, an interpolation method between two sets X and Y must gradually remove features from X and gradually incorporate features from Y . The features in $X \cap Y$ must remain unchanged. Taking this heuristic into account, to calculate the interpolates between X and Y , one can calculate the interpolates between X and $X \cap Y$, $\{U_\alpha\}$, and interpolates between Y and $X \cap Y$, $\{W_\alpha\}$. Then the interpolates between X and Y are given by, $\{Z_\alpha\}$, where,

$$Z_\alpha = U_{1-\alpha} \cup W_\alpha \quad (22)$$

Thus we need only develop a method to calculate the median between X and Y under the assumption $X \subseteq Y$, and any such method extends to the general case using (22).

To assess the reasonability of the above simplification, consider the case when the interpolates U_α and W_α are obtained by definition 2. Then, the following can be easily obtained from definitions.

$$\begin{aligned} d(X, U_\alpha) &= (1-\alpha)\rho_1 & d(X \cap Y, U_\alpha) &= (\alpha)\rho_1 \\ d(Y, W_\alpha) &= (1-\alpha)\rho_2 & d(X \cap Y, W_\alpha) &= (\alpha)\rho_2 \\ U_\alpha &\subset X & W_\alpha &\subset Y \end{aligned}$$

Here we assumed that $d(X, X \cap Y) = \rho_1$ and $d(Y, X \cap Y) = \rho_2$. Also, assume without loss of generality that $\rho_1 < \rho_2$. Then the proposition 2 holds true.

Proposition 2. *Let $\{U_\alpha\}$ and $\{W_\alpha\}$ be as described above. Let the interpolates be defined by (22). Then we have*

$$d(X, Z_{0.5}) = d(Y, Z_{0.5}) = 0.5 * \rho_2 \quad (23)$$

Proof. Firstly note that,

$$\begin{aligned} \bar{d}(X, Z_\alpha) = \bar{d}(X, W_\alpha) &\leq \bar{d}(X \cap Y, W_\alpha) = \alpha\rho_2 \\ \bar{d}(Z_\alpha, X) &\leq \bar{d}(U_\alpha, X) = (1-\alpha)\rho_1 \end{aligned}$$

Hence we have,

$$d(X, Z_\alpha) \leq \sup\{\alpha\rho_2, (1-\alpha)\rho_1\} \quad (24)$$

Similarly, we can also deduce that

$$d(Y, Z_\alpha) \leq \sup\{\alpha\rho_1, (1-\alpha)\rho_2\} \quad (25)$$

Considering the case when $\alpha = 0.5$ with the assumption that $\rho_1 < \rho_2$, we can prove equation 23. \square

The proposition 2 is stated to justify the reasonability of the method to construct interpolates. In other words, proposition 2 implies that **if interpolates are constructed to satisfy property as in (15), then the construction as described above preserves this property.**

3) *Construct only medians:* Any $\alpha \in [0, 1]$ can be written in binary code. Thus, if one has a method to generate only the interpolate $Z_{0.5}$, one can generate the interpolate for any α . For example, let $\alpha = 5/8$. The following steps would generate Z_α .

- (i) Generate interpolate between Z_0 and Z_1 , we get $Z_{0.5}$.
- (ii) Generate interpolate between $Z_{0.5}$ and Z_1 , we get $Z_{0.75}$.
- (iii) Generate interpolate between $Z_{0.5}$ and $Z_{0.75}$, we get $Z_{0.625} = Z_\alpha$.

The interpolate $Z_{0.5}$ is referred to as the *median* interpolate. Thus, if one has the method to generate the median interpolate, one can generate the interpolate for any α . However, note that any such method to produce the median must satisfy the consistency property 1. In simplest case this means - the median between $Z_{0.25}$ and $Z_{0.75}$ must equal the median between Z_0 and Z_1 .

Property 1 (Consistency of Median). *Let Z_{α_1} and Z_{α_2} be two interpolates. Then the median between Z_{α_1} and Z_{α_2} must be $Z_{(\alpha_1+\alpha_2)/2}$*

Proposition 3. *Suppose $X \subseteq X' \subseteq Y' \subseteq Y$ and $m(X, Y)$ denotes the median between X and Y then*

$$m(X, Y) = m(X', Y') \Rightarrow m(X, Y) = m(m(X, X'), m(Y, Y')) \quad (26)$$

if (26) holds true and we have that

$$m(Z_0, Z_1) = m(Z_{0.25}, Z_{0.75}) \quad (27)$$

then the property 1 holds as well.

Proof. Here we only provide the intuitive idea of why the proposition is correct. Let $Z_0 = X \subset Y = Z_1$. Indicate the median, $m(Z_{\alpha_1}, Z_{\alpha_2})$ by $Z_{(\alpha_1+\alpha_2)/2}$. Thus $Z_{0.5} = m(Z_0, Z_1)$. Assume that,

$$Z_{0.5} = m(Z_{0.25}, Z_{0.75}) = m(Z_0, Z_1) = m(Z_{0.5}, Z_{0.5}) \quad (28)$$

Using (26) we get,

$$Z_{0.5} = m(Z_{0.125}, Z_{0.875}) = m(Z_0, Z_1) = m(Z_{0.375}, Z_{0.625}) \quad (29)$$

One can continue this to show that, for all $\epsilon < 0.5$

$$Z_{0.5} = m(Z_{0.5-\epsilon}, Z_{0.5+\epsilon}) \quad (30)$$

This can be generalized to any α , that is

$$Z_\alpha = m(Z_{\alpha-\epsilon}, Z_{\alpha+\epsilon}) \quad (31)$$

by observing that sets X and Y are arbitrary. So, the first time we encounter α , we can name the sets Z_0 and Z_1 and proceed accordingly. \square

Note that consistency of the medians is a desired property. However, the heuristic is still valid and can be followed to reduce the computational costs.

B. Median

In [4] the definition 3 of median is proposed.

Definition 3 (Median). *Given two sets $X \subseteq Y$, the median $m(X, Y)$ is defined as*

$$m(X, Y) = \bigcup_{\lambda \geq 0} (\{X \oplus \lambda B\} \cap \{Y \ominus \lambda B\}) \quad (32)$$

The medians defined above can also be characterized in terms of influence zones as shown in proposition 4.

Proposition 4. *Let $X \subseteq Y$ be two sets and B be the circular structuring element. Let the median be defined as in (32). Then we have that*

$$m(X, Y) = IZ(X | Y^c) \quad (33)$$

Proof. We have

$$\begin{aligned} IZ(X | Y^c) &= \bigcup_{\lambda} \{(X \oplus \lambda B) \cap (Y^c \oplus \lambda B)^c\} \\ &= \bigcup_{\lambda} \{(X \oplus \lambda B) \cap (Y \ominus \lambda B)\} \\ &= m(X, Y) \end{aligned}$$

The first equality follows from (12) The second equality comes from the duality between dilation and erosion operators. \square

Another property we expect from such a median is *duality*. That is, we expect that $m(X, Y) = (m(Y^c, X^c))^c$ to hold. The medians do not satisfy this property, but one can show that they are ‘‘close enough’’. The dual median is defined as

$$M(X, Y) = (m(X^c, Y^c))^c \quad (34)$$

Proposition 5. *Let $X \subseteq Y$ be two sets. Let $m(X, Y)$ be the median as defined in (32). Let $M(X, Y)$ be the dual median as defined in (34). Then we have*

$$M(X, Y) = \bigcap_{\lambda > 0} \{(Y \ominus \lambda B) \cup (X \oplus \lambda B)\} \quad (35)$$

and

$$M(X, Y) \setminus m(X, Y) = \{x | d(x, X) = d(x, Y)\} \quad (36)$$

Proof. Equation (35) can be obtained by set transformations. To show (36) - Since, we have that, from proposition 4.

$$m(X, Y) = IZ(X | Y^c) = \{x | d(x, X) < d(x, Y^c)\}$$

and

$$\begin{aligned} M(X, Y) &= (m(X^c, Y^c))^c \\ &= (IZ(Y^c | X))^c = \{x | d(x, Y^c) < d(x, X)\}^c \\ &= \{x | d(x, X) \leq d(x, Y^c)\} \end{aligned}$$

Thus although, duality does not hold, we have that the median and the dual median only differ in the boundary.

Recall that we have stated earlier that it is favorable for medians to satisfy the consistency property 1. Although, the medians defined above satisfy this property for simple sets, it is still an open question as to whether it is true for all sets $X \subseteq Y$. We discuss further on this in the section (refer).

Another problem with the medians arises in the case of non-convex shapes. Consider the sets X and Y as in figure 5 (a) and (b). One expects the median to be close to figure 5(e) while the median calculation results in 5(c).

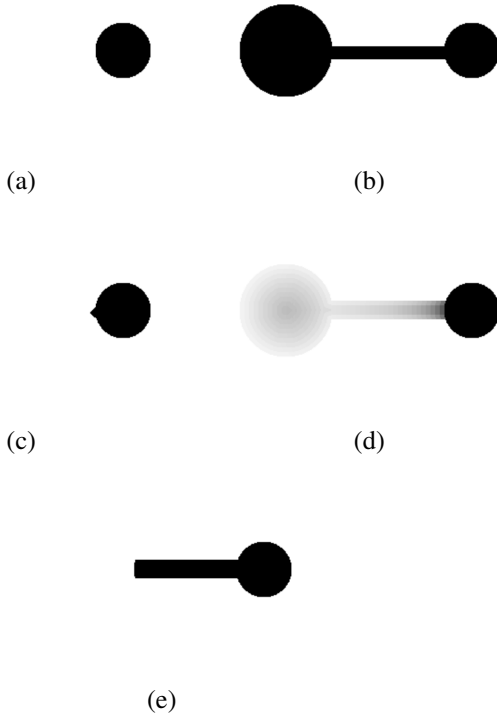


Fig. 5. (a) Set X . (b) Set Y (c) The median calculated according to (32). (d) The grey scale image obtained by Meyer's method. (e) Median calculated using the proposed approach (37).

There is however a simple solution to this issues. Assume that $X \subseteq Y$. Let $\bar{d}(X, Y) = \rho$. For all $x \in Y \setminus X$. Define

$$f(x) = \begin{cases} 1 & x \in X \\ 1 - \frac{d_\delta(X, x)}{\rho} & x \in Y \setminus X \\ 0 & x \in Y^c \end{cases} \quad (37)$$

Thresholding the greyscale image in (37) gives the interpolates. This method is first described in the article [14]. This method works better in such cases. The median image in figure 5(e) is obtained using this method.

C. Meyer's Method

We now describe yet another method to calculate the interpolates between two images, due to F. Meyer, as described in [3]. Given two sets X and Y , we are required to find a median.

□ As mentioned earlier, we assume that $X \subseteq Y$. Let x be a point in the set $Y \setminus X$. Let $d_\delta(X, x) = \inf\{\lambda \mid x \in X \oplus \lambda B\}$, and $d_\epsilon(x, Y) = \inf\{\lambda \mid x \notin Y \ominus \lambda B\}$. Define

$$f(x) = \begin{cases} 1 & x \in X \\ \frac{d_\epsilon(x, Y)}{d_\epsilon(x, Y) + d_\delta(X, x)} & x \in Y \setminus X \\ 0 & x \in Y^c \end{cases} \quad (38)$$

We thus have a greyscale image with values in $[0, 1]$. To calculate the interpolate, we take

$$Z_\alpha = \mathbb{T}_\alpha(f) \quad (39)$$

where, $\mathbb{T}_\alpha(\cdot)$ is a threshold operator and f is the greyscale image obtained by (38). This formulation gives us an easy and efficient way to calculate the medians. An example is shown in figure 5(d).

Proposition 6. *Let $X \subseteq Y$ be two sets. The median calculated by (32), is the same as one obtained by (39), taking $\alpha = 0.5$.*

Proof. The proof follows from the fact that, at $\alpha = 0.5$ we have that the median consists of

$$\{x : d_\delta(X, x) \leq d_\epsilon(x, Y)\} \quad (40)$$

In other words, the Meyer's median is equal to $IZ(X|Y^c)$, which from proposition 4 equals the one in (32). □

Note that although the median elements for both Meyer's method and median obtained by (32) are the same, in general this need not be true for all interpolates.

The main advantage of Meyer's method is that one can calculate all the interpolates at one shot and this saves a lot of computation.

V. GREYSCALE IMAGES

Recall that the operators of binary images are extended to greyscale images using subgraphs. An important point to note is that not all the three dimensions can be treated the same. Two dimensions belong to the spatial domain, and the third gives the value domain. This impacts the way structuring elements would be handled. This results in two kinds of structuring elements - flat and non-flat as discussed in II-B. In this section we first look at how the interpolation methods discussed above extend to greyscale images. We then analyze the distinction between flat and non-flat structuring elements.

Firstly, note that simply replacing the binary dilation/erosion with greyscale dilation/erosion will enable to extend the interpolations in definitions 1 and 2 to greyscale images as well. Since greyscale images are just sets (subgraphs) in a different space, all the properties generalize accordingly.

For the median calculation in definition 3, one needs to verify if the series of simplifications in section IV-A are still valid. The assumption 1, $X \cap Y \neq \emptyset$ trivially holds for greyscale images since we consider the subgraphs. This is because of having a value domain. Assumption 2, $X \subset Y$ also holds for greyscale images, since we still are considering sets, although in higher dimensions. Assumption 3, that medians are enough, also would apply greyscale images. Thus, if f_1 and f_2 are two 1-d greyscale images, we assume that $f_1 \geq f_2$ and the problem of interpolation drops to finding the median element.

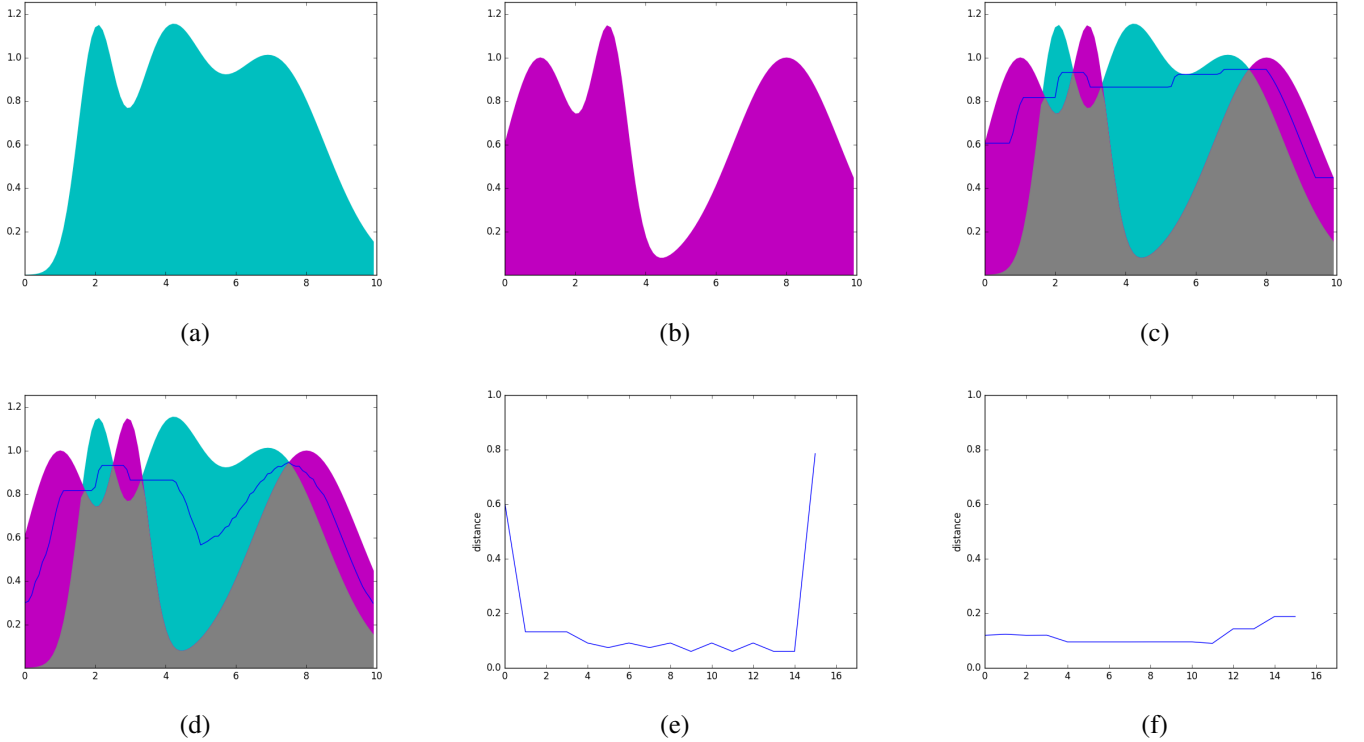


Fig. 6. (a) Shoreline at time $t = 0$ denoted by the cyan region. (b) Shoreline at time $t = 1$ denoted by the cyan region. The grey region indicates the part which did not change between times $t = 0$ and $t = 1$. (c) Median (boundary) obtained by flat structuring element indicated by the blue line. (d) Median (boundary) obtained by non-flat structuring element indicated by the blue line. (e) Plot of the distances as in (42) between successive interpolates obtained by flat structuring element. (f) Plot of the distances as in (42) between successive interpolates obtained by non-flat structuring element.

A. Flat vs Non-Flat structuring elements

A point to note is that, in binary images we are assured of getting thin interpolates using influence zones. This extends to greyscale images as well only if we use non-flat structuring elements. Thin interpolates are not assured if we use flat structuring elements, and this is the reason why the practice is to take non-flat structuring elements is followed. However, a transformation on the value domain would allow us to obtain thin interpolates.

Proposition 7. *Let $f_1(x) \geq f_2(x)$ for all x , be two greyscale images defined on finite domain $E \subset \mathbb{R}^2$. If, $\inf f_1 \leq \sup f_2$, then $SKIZ(f_2, f_1^c)$ has the measure 0, when influence zones are calculated using flat structuring elements.*

We only provide an intuitive explanation for the proposition. Intuitively, for greyscale images, $SKIZ$ consists of all the points which are equidistant to the two sets and also all the points which cannot be reached by either of them by any number of finite dilations (usually happens for flat structuring elements). However, in case we have $\inf f_1 \leq \sup f_2$, then the latter situation does not arise and hence the $SKIZ$ is thin.

The above proposition implies that under some conditions, thick boundaries do not appear even with flat structuring elements. It is not tough to see that, there exists a transformation on the value domain, under which one can guarantee $\inf f_1 \leq \sup f_2$. Note that this transformation results in the changes to brightness and contrast in an image. We assume

that whenever the method uses flat structuring elements, this transformation is suitably applied.

In summary, the procedure to calculate the median according to definition 3 is

- 1) Let f_1 and f_2 be two greyscale images.
- 2) Calculate $\hat{f} = \min(f_1, f_2)$.
- 3) Calculate the medians between f_1 and \hat{f} , $\{x_\alpha\}$ and f_2 and \hat{f} , $\{y_\alpha\}$. If using flat structuring elements, appropriately scale f_1 and f_2 .
- 4) The median between f_1 and f_2 is then given by $\max(x_\alpha, y_\alpha)$.
- 5) Repeat the above steps iteratively to get the interpolates.

Which to choose- Flat or Non-Flat? Usually, Non-flat structuring elements are preferred since they do not result in “thick” interpolates. However, the proposition 7 states that even flat structuring elements do not result in “thick” interpolates under some conditions. In practice, it has been observed that non-flat structuring elements gives “smoother” interpolates.

1) Example: Simulated shoreline interpolation: As an example to illustrate the difference between flat and non-flat structuring elements, we simulate shorelines at two distinct times and calculate the interpolates. Evolving shorelines has also been studied in [15], using medians to extrapolate the shorelines.

We simulate the shorelines by considering two 1-

dimensional functions

$$\begin{aligned} f_1 &= N(2, 0.5) + N(4, 1) + N(7, 1.5) \\ f_2 &= N(1, 1) + N(3, 0.5) + N(8, 1.5) \end{aligned}$$

where,

$$N(\mu, \sigma) = \exp\left\{\frac{1}{2}\left(\frac{x - \mu}{\sigma}\right)^2\right\} \quad (41)$$

The functions f_1 and f_2 are shown in figures 6 (a) and (b). The median obtained by flat/non-flat structuring elements is plotted in figures 6 (c) and (d) respectively. It can be seen that the median calculated using non-flat structuring element takes into account the shape of f_1 better than the median using flat structuring element, between 4 and 8. This is because, in that patch the flat structuring element cannot go below the minimum. This in effect shows that proposition 7 is not enough to justify the use of flat structuring elements instead of non-flat structuring elements.

$$L^\infty(f_1, f_2) = \sup_x |f_1(x) - f_2(x)| \quad (42)$$

To analyze the difference further, hierarchical medians were generated to the level 4 (which gives 16 interpolates in total) for both flat and non-flat structuring elements. Then distance measured by L^∞ (42) is calculated between successive interpolates and plotted in figures 6 (c) and (d). From this, one can deduce that non-flat structuring elements gives smoother interpolates compared to the flat structuring elements.

VI. EXTENSIONS AND FUTURE WORK

As stated earlier, another important aim of this paper is to provide a platform for various extensions and future work. In this section, we pose several questions and discuss possible questions to be answered.

A. Graph based Interpolation

A graph $\mathcal{G} = (V, E)$ is a tuple of a vertex set V and an edge set $E \subseteq V \times V$. An image can be represented as a graph, taking the set of pixels as the vertex set and edges between two adjacent pixels. Recently, MM operators are generalized to graphs [16], [17], [18]. So, a natural question arises - Can we extend the morphological interpolates to graphs as well? We briefly review the question here.

The basic MM operators, dilation and erosion, can be extended to the graphs using the lattice definitions - dilation defined as the operator which preserves the supremum and erosion being the operator which preserves the infimum. There are in fact two different kinds of dilations/erosions one can define - $\delta^\bullet, \delta^\times, \epsilon^\bullet, \epsilon^\times$. (Complete details can be found in [16]). The operators $\delta^\bullet, \epsilon^\bullet$ map the set of edges to a set of vertices while the operators $\delta^\times, \epsilon^\times$ map a set of vertices to a set of edges.

Defining,

$$\begin{aligned} \Delta(X) &= \delta^\bullet(\delta^\times(X)) \\ \mathcal{E}(X) &= \epsilon^\bullet(\epsilon^\times(X)) \end{aligned}$$

allows us to define the dilation and erosion operators on the set of vertices to vertices. All the above methods to obtain binary interpolates can be directly extended to graphs using these operators instead.

There is also another possibility of extending the operators using only δ^\times or δ^\bullet . Each of these operators can be thought of as half-dilations. To represent these, one has to use a different representation of the image using *cubical complexes* as established in [19].

For greyscale images, one can think of them as binary images in higher dimension, construct the graph and then proceed as above. However, an alternate solution would be to extend the graph based MM operators to weighted graphs and accordingly define the interpolates. The topic of analyzing the graph based interpolations and greyscale operators on graphs is left as a topic of further research.

B. Problem of median being consistent

Recall that in property 1 we stated that any median must be consistent, and in proposition 3 we have given an equivalent condition for the property to hold. It can be easily seen that the median obtained by using (37) follows this property. However, it still an open question whether medians proposed in definition 3 satisfies this property or not. Apart from this, other equivalent conditions to the consistency property 1 might provide better insights into the interpolation problem.

C. Metric for judging interpolates

An important task is to have an ability of judging interpolates obtained via a metric. This would allow us to compare different methods of interpolation and maybe obtain new interpolation methods as well. The basic criteria for such a metric is

- It should have higher values for non-smooth interpolates compared to smoother interpolates
- Should be independent of the number of interpolates obtained.

As a starting point, one can consider the following metric. Let $d(I_1, I_2)$ be any metric to measure the distance between two images. For example L^∞ measure. Let $\mathcal{Z} = \{I_0 = Z_0, Z_1, Z_2, \dots, Z_n = I_1\}$ be a set of interpolates. Define,

$$D(\mathcal{Z}) = \sup_{0 < i < n-1} d(Z_i, Z_{i+1}) \quad (43)$$

This satisfies the condition to penalize non-smooth interpolates. However, increasing the number of interpolates can reduce this metric. Finding a right metric to judge interpolates is also a subject of future research.

D. Interpolation as a optimization problem

A time tested way of solving a problem is to pose it as an optimization problem. This makes the problem well-defined and allows us to techniques from other areas to calculate the interpolates. This can be considered as one of the topics of further research.

VII. CONCLUSION

In this article we reviewed a method to get the solution to the problem of image interpolation - Given two images I_1 and I_2 find the suitable intermediate images. We have reviewed the basic methods for morphological interpolations from the view of geoscience and remote sensing, and provided a theoretical consolidation of various ideas available in the literature. Apart from this, we have also stated and discussed briefly several problems and directions for future work.

VIII. ACKNOWLEDGEMENTS

We would like to thank Prof. Jean Serra for his help. The authors AC and SD would like to thank Indian Statistical Institute for the fellowship provided to pursue the research. BSDS would like to acknowledge the support received from the Indian Space Research Organization (ISRO) with the grant number ISRO/SSPO/Ch-1/2016-17.

REFERENCES

- [1] B.S.D. Sagar, "Visualization of spatiotemporal behavior of discrete maps via generation of recursive median elements," *Pattern Analysis and Machine Intelligence, IEEE Transactions on*, vol. 32, no. 2, pp. 378–384, 2010.
- [2] J Serra and P Soille, *Mathematical morphology and its applications to image processing*, vol. 2, Springer Science & Business Media, 2012.
- [3] F Meyer, "A morphological interpolation method for mosaic images," in *Mathematical Morphology and its Applications to Image and Signal Processing*, pp. 337–344. Springer, 1996.
- [4] J. Serra, "Hausdorff distances and interpolations," *Computational Imaging and Vision*, vol. 12, pp. 107–114, 1998.
- [5] V Chatzis and I Pitas, "Interpolation of 3-d binary images based on morphological skeletonization," *IEEE transactions on medical imaging*, vol. 19, no. 7, pp. 699–710, 2000.
- [6] D N Vizireanu, S Halunga, and O Fratu, "A grayscale image interpolation method using new morphological skeleton," in *Telecommunications in Modern Satellite, Cable and Broadcasting Service, 2003. TELSIKS 2003. 6th International Conference on*. IEEE, 2003, vol. 2, pp. 519–521.
- [7] J. Serra, *Image Analysis and Mathematical Morphology*, Academic Press, Inc., Orlando, FL, USA, 1983.
- [8] L. Najman and H. Talbot, *Mathematical morphology*, John Wiley & Sons, 2013.
- [9] G. Matheron, *Random sets and integral geometry*, Wiley series in probability and mathematical statistics: Probability and mathematical statistics. Wiley, 1975.
- [10] G. Birkhoff, *Lattice Theory*, Number v. 25, pt. 2 in American Mathematical Society colloquium publications. American Mathematical Society, 1940.
- [11] G. Grätzer, *Lattice Theory: Foundation*, SpringerLink : Bücher. Springer Basel, 2011.
- [12] M. Iwanowski and J. Serra, "The morphological-affine object deformation," in *Mathematical Morphology and its Applications to Image and Signal Processing*, pp. 81–90. Springer, 2000.
- [13] S. Beucher, "Sets, partitions and functions interpolations," *Computational Imaging and Vision*, vol. 12, pp. 307–314, 1998.
- [14] A Challa, S Danda, and B S D Sagar, "Morphological interpolation for temporal changes," in *Geoscience and Remote Sensing Symposium (IGARSS), 2016 IEEE International*. IEEE, 2016, pp. 3358–3361.
- [15] J Serra, "Shoreline extrapolations," *Hornická přibram ve vědě a technice*, 2011.
- [16] J Cousty, L Najman, F Dias, and J Serra, "Morphological filtering on graphs," *Computer Vision and Image Understanding*, vol. 117, no. 4, pp. 370–385, 2013.
- [17] HJAM Heumans, P Nacken, A Toet, and L Vincent, "Graph morphology," *Journal of visual communication and image representation*, vol. 3, no. 1, pp. 24–38, 1992.
- [18] L Najman and J Cousty, "A graph-based mathematical morphology reader," *Pattern Recognition Letters*, vol. 47, pp. 3–17, 2014.
- [19] E Khalimsky, R Kopperman, and P R Meyer, "Computer graphics and connected topologies on finite ordered sets," *Topology and its Applications*, vol. 36, no. 1, pp. 1–17, 1990.



Aditya Challa received the B.Math.(Hons.) degree in Mathematics from the Indian Statistical Institute - Bangalore, and Masters in Complex Systems from University of Warwick, UK - in 2010, and 2012, respectively. From 2012 to 2014, he worked as a Business Analyst at Tata Consultancy Services, Bangalore. In 2014, he joined as a Junior Research Fellow at Indian Statistical Institute - Bangalore, where he is currently a Senior Research Fellow in the Systems Science and Informatics Unit. His current research interests focus on the solutions to the Image Interpolation Problem, and using techniques from Mathematical Morphology in Data Mining.



Sravan Danda received the B.Math.(Hons.) degree in Mathematics from the Indian Statistical Institute - Bangalore, and the M.Stat. degree in Mathematical Statistics from the Indian Statistical Institute - Kolkata, in 2009, and 2011, respectively. From 2011 to 2013, he worked as a Business Analyst at Genpact - Retail Analytics, Bangalore. In 2013, he joined as a Junior Research Fellow at Indian Statistical Institute - Bangalore, where he is currently a Senior Research Fellow in the Systems Science and Informatics Unit under the joint supervision of B.S.Daya Sagar and

Laurent Najman. His current research interests focus on the development of tools for Image filtering and segmentation using combinatorial optimization and Discrete Mathematical Morphology.



B. S. Daya Sagar (M03-SM03) received the M.Sc and Ph.D degrees from the Faculty of Engineering, Andhra University, Visakhapatnam, India, in 1991 and 1994 respectively. Sagar is currently a Professor at Systems Science and Informatics Unit (SSIU) of Indian Statistical Institute Bangalore Centre, India. He is also the first Head of the SSIU. Earlier, he worked in College of Engineering, Andhra University, and Centre for Remote Imaging Sensing and Processing (CRISP), The National University of Singapore in various positions during 1992-2001. He

served as Associate Professor and Researcher in the Faculty of Engineering and Technology (FET), Multimedia University, Malaysia during 2001-07. His research interests include mathematical morphology, GISci, digital image processing, fractals and multifractals and their applications in extraction, analyses, and modeling of geophysical patterns. He has published over 75 papers in journals, and has authored and/or guest edited 9 books and/or special theme issues for journals. He recently authored a book entitled "Mathematical Morphology in Geomorphology and GISci" CRC Press: Boca Raton, 2013, p.546. He recently co-edited a special issue on "Filtering and Segmentation with Mathematical Morphology" for IEEE Journal on Selected Topics in Signal Processing (v. 6, no. 7, p. 737-886, 2012). He is an elected Fellow of Royal Geographical Society (1999), Indian Geophysical Union (2011), and was a member of New York Academy of Science during 1995-96. He received the Dr. Balakrishna Memorial Award from Andhra Pradesh Academy of Sciences in 1995, Krishnan Gold Medal from the Indian Geophysical Union in 2002, and "Georges Matheron Award-2011 (with Lecturership)" of the International Association for Mathematical geosciences. He is the Founding Chairman of Bangalore Section of the IEEE GRSS Chapter. He is on the Editorial Boards of Computers and geosciences, and Frontiers: Environmental Informatics.



Laurent Najman received the Habilitation à Diriger les Recherches in 2006 from University the University of Marne-la-Vallée, a Ph.D. of applied mathematics from Paris-Dauphine University in 1994 with the highest honor (Flicitations du Jury) and an “Ingénieur” degree from the Ecole des Mines de Paris in 1991. After earning his engineering degree, he worked in the central research laboratories of Thomson-CSF for three years, working on some problems of infrared image segmentation using mathematical morphology. He then joined a

start-up company named Animation Science in 1995, as director of research and development. The technology of particle systems for computer graphics and scientific visualization, developed by the company under his technical leadership received several awards, including the “European Information Technology Prize 1997” awarded by the European Commission (Esprit programme) and by the European Council for Applied Science and Engineering and the “Hottest Products of the Year 1996” awarded by the Computer Graphics World journal. In 1998, he joined Océ Print Logic Technologies, as senior scientist. He worked there on various problem of image analysis dedicated to scanning and printing. In 2002, he joined the Informatics Department of ESIEE, Paris, where he is professor and a member of the Institut Gaspard Monge, Université Paris-Est Marne-la-Vallée. His current research interest is discrete mathematical morphology.